Breakup reaction studies of ^{10}Be and ^{10,11}B using a ^{10}Be beam

S. Ahmed,[1] M. Freer,[1] J. C. Angélique,[3] N. I. Ashwood,[1] V. Bouchat,[4] W. N. Catford,[2,3] N. M. Clarke,[1] N. Curtis,[1] F. Hanappe,[4] J. C. Lecouey,[3,*] F. M. Marqués,[3] T. Materna,[4] A. Ninane,[7] G. Normand,[3] N. A. Orr,[3] S. Pain,[2] N. Soić,[1,†] C. Timis,[3,‡] A. Unshakova,[5] and V. A. Ziman[1]

[1]*School of Physics and Astronomy, University of Birmingham, Edgbaston, Birmingham, B15 2TT, United Kingdom*
[2]*School of Electronics and Physical Sciences, University of Surrey, Guildford, Surrey GU2 7XH, United Kingdom*
[3]*Laboratoire de Physique Corpusculaire, ISMRA and Universite de Caen, IN2P3-CNRS, 14050 Caen Cedex, France*
[4]*Université Libre de Bruxelles, Case Pastale 226, B-1050 Bruxelles, Belgium*
[5]*Joint Institute for Nuclear Research, 141980 Dubna, Moscow Region, Russia*
[6]*Institute de Researches Subatomique, IN2P3-CNRS/Université Louis Pasteur, Boîte Postale 28, 67037 Strasbourg Cedex, France*
[7]*Institut de Physique, Université Catholique de Louvain, Louvain-la-Neuve, Belgium*

(Received 29 August 2003; published 12 February 2004)

The structure of ^{10}Be has been investigated by inelastic scattering to states above the breakup threshold using the reaction ^{12}C(^{10}Be, ^{10}Be$^{*}\rightarrow{}^{6}$He+^{4}He)^{12}C at $E_{beam}=302$ MeV. Excited states in ^{10}Be were observed at 9.6 ± 0.1 and 10.2 ± 0.1 MeV. No evidence was observed for the population of the 4^{+} member of the ground-state band of ^{10}Be indicating the shell-model-like structure of the ground state. In addition, the decay of ^{8}Be, ^{10}B, and ^{11}B, populated in the two-neutron, proton pickup, breakup and $1p$ pickup reactions, was reconstructed through the detection of coincident ^{4}He+^{4}He, ^{4}He+^{6}Li, and ^{4}He+^{7}Li particles. Cross sections for the formation of the ^{8}Be, ^{9}Be, ^{10}B, and ^{11}B were also deduced. Contrary to expectations, the two-neutron removal results in the production of ^{8}Be predominantly (80%) in the first excited (2^{+}) state. This suggests that dynamical excitations play an important role in the neutron removal process.

DOI: 10.1103/PhysRevC.69.024303 PACS number(s): 21.10.−k, 21.60.−n, 25.70.−z, 27.20.+n

I. INTRODUCTION

The spectroscopy of light neutron-rich nuclei has been the focus of considerable interest in a bid to understand the evolution in structural properties between stability and the neutron dripline. In particular, the beryllium isotopes offer a rather convenient system in which to perform such studies, given that it is one of the few isotopic chains which may be probed at the limits with appreciable secondary beam intensities. Moreover, the Be isotopes exhibit a number of exotic structural modes. For example, ^{11}Be has long been characterized as a single-neutron halo, and owing to the strong influence of the 2α cluster structure of ^{8}Be, the neutron-rich isotopes have been identified with molecularlike characteristics [1,2]. The nature of the low-lying states of ^{9}Be is well described by such a picture. The nucleus of ^{10}Be, however, continues to be the subject of experimental investigation in order to determine the character of the states above the excitation energy of 6 MeV, a region in which molecular or cluster structures are theoretically predicted to occur [1–5]. Recently, measurements of the structure of states in ^{10}Be in this energy region have been performed using the ^{6,7}Li(^{7}Li, ^{4}He+^{6}He) reactions [6,7], single-neutron transfer ^{9}Be(^{9}Be, ^{10}Be)^{8}Be [8], two-proton transfer ^{12}C(^{15}N, ^{17}F)^{10}Be [9], and also two-neutron removal ^{12}C(^{12}Be, ^{10}Be)^{14}C [10]. In addition, the α-particle decay widths of the 7.54-MeV and 9.6-MeV states have been measured [11]. These measurements provide a better understanding of the $E_{x}>6$ MeV region, however, the picture is not yet complete.

In the present paper we report on a measurement, using a high-energy (30 MeV/nucleon) ^{10}Be beam, of the inelastic scattering to α-decaying states in a region of excitation in which molecular structures are believed to play an important role. In addition, we report on measurements of the α breakup of ^{10,11}B excited states populated in transfer reactions, the structure of which are linked to states in ^{10}Be. Finally, we report a measurement of the two-neutron removal reaction leading to ^{8}Be, where using the invariant mass spectroscopic method we have reconstructed the ^{8}Be core states.

II. EXPERIMENTAL TECHNIQUES

A 302 MeV ^{10}Be secondary beam with an intensity of 10^{4} particles per second (constrained by detector rate limits) was produced from the reaction of a 60 MeV/nucleon ^{13}C primary beam, provided by the GANIL accelerator facility, on a Be target. The spread in the beam energy was <1 MeV due to the constrained momentum acceptance required to limit the beam intensity. The reaction products were analyzed by the LISE3 magnetic spectrometer, in terms of mass, charge, and momentum, which allowed beam purification to ~95%. The secondary beam was focussed onto a 20 mg/cm^{2} carbon target and was tracked event by event onto the target using two x-y position-sensitive drift chambers, which provided a measurement of the position of the beam on the target with a

*Present address: NSCL, Michigan State University, Michigan 48824, USA.
†Present address: Rudjer Bošković Institute, Department of Experimental Physics, Bijenička 54, HR-10000 Zagreb, Croatia.
‡Present address: School of Electronics and Physical Sciences, University of Surrey, Guildford, Surrey, GU2 7XH, UK.

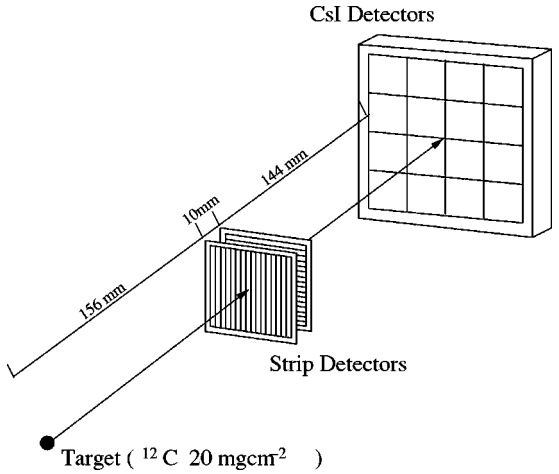

FIG. 1. A schematic diagram of the experimental setup of the charged fragment detectors. Note that the Si strip and CsI detectors are aligned along the beam axis and positioned such that the same solid angle is subtended for each detector. Not to scale.

resolution [full width at half maximum (FWHM)] of ~1 mm and the incident angle to within 1°. The breakup products were detected using a multielement Si-CsI telescope aligned with the beam axis. The Si elements were placed ~17 cm from the target, and consisted of two 500 μm-thick 5×5-cm^2 position-sensitive strip detectors (PSSDs), with the front detector surface divided into 16 independent vertical position-sensitive strips, each strip 5 cm long and 0.3 cm wide and the back PSSD divided into 16 horizontal strips. These two detectors were backed by an array of 16, 2.5×2.5 cm^2, CsI scintillator detectors, with an energy resolution (FWHM) of the order of 1.5%, situated ~30 cm from the target so as to subtend the same solid angle as the silicon detectors. Figure 1 shows a schematic illustration of the arrangement of the Si and CsI detectors. The energy and position resolutions of the PSSDs were 200 keV and 1 mm, respectively. The telescope was centered at 0° with respect to the beam axis and subtended an angular range of 0°–11.95° (to the farthest corner of the second strip detector) with respect to this axis. The detector positions and energy responses were determined using a mixed-isotope α-calibration source (consisting of ^{239}Pu, ^{241}Am, and ^{244}Cm) and a mixed beam of light ions of known energies produced using the ^{13}C beam. The ^{4}He, ^{6}He, ^{6}Li, and ^{7}Li secondary reaction products were identified unambiguously from the characteristic energy losses in the Si-CsI telescopes.

The study of the structure of light nuclei using breakup reactions has a number of advantages, particularly for situations in which the projectile is a secondary beam produced via in-flight fragmentation. Thick targets are used to compensate for the typically low intensities. However, the use of such targets degrades the resolution with which the spectroscopy of the reaction products may be explored. Breakup reactions, in which the excitation energy of the unbound state is determined by the relative velocity of the decay products, tend to suffer less from the effects of energy and angular straggling in the target owing to the lower nuclear charges of the products (for near symmetric breakup). Furthermore, the effects of large beam spots cancel to a large extent in the determination of the calculation of the excitation energy of the resonant particle. In the present instance the two-body breakup reaction channels $^{10}\mathrm{Be}\rightarrow{}^4\mathrm{He}+{}^6\mathrm{He}$, $^8\mathrm{Be}\rightarrow{}^4\mathrm{He}+{}^4\mathrm{He}$, $^{10}\mathrm{B}\rightarrow{}^4\mathrm{He}+{}^6\mathrm{Li}$, and $^{11}\mathrm{B}\rightarrow{}^4\mathrm{He}+{}^7\mathrm{Li}$ were investigated here. The decay thresholds for the various decay processes are shown in Table I. With the exception of the decay threshold of ^{8}Be which lies 92 keV below the ground state, the thresholds for the various channels are of the same order, which suggest that states in the same excitation energy region should be observed. Monte Carlo simulations of the geometry and the response of the detection system indicate that the efficiency for the breakup of the ^{10}Be nucleus into $^4\mathrm{He}+{}^6\mathrm{He}$ fragments was between 40% and 50%. This efficiency was typical of the other breakup reactions studied here, i.e., $^{10}\mathrm{B}\rightarrow{}^4\mathrm{He}+{}^6\mathrm{Li}$, $^{11}\mathrm{B}\rightarrow{}^4\mathrm{He}+{}^7\mathrm{Li}$, and $^8\mathrm{Be}\rightarrow{}^4\mathrm{He}+{}^4\mathrm{He}$ (the efficiency for the decay to the 0^+ ground state in ^{8}Be was 22%).

TABLE I. Decay thresholds for the four reaction channels observed in the present measurements.

Decay channel	Threshold (MeV)
$^{10}\mathrm{Be}\rightarrow{}^4\mathrm{He}+{}^6\mathrm{He}$	7.409
$^{10}\mathrm{Be}\rightarrow{}^4\mathrm{He}+{}^4\mathrm{He}+2n$	8.48
$^8\mathrm{Be}\rightarrow{}^4\mathrm{He}+{}^4\mathrm{He}$	−0.092
$^{10}\mathrm{B}\rightarrow{}^4\mathrm{He}+{}^6\mathrm{Li}$	4.459
$^{11}\mathrm{B}\rightarrow{}^4\mathrm{He}+{}^7\mathrm{Li}$	8.663

III. RESULTS

The kinematics of the breakup were reconstructed using the resonant particle spectroscopy method [12,13]. By measuring the masses, momenta, angles, and thus relative velocities of the fragments, for three-body reactions, the energy of the unobserved particle may be deduced via momentum conservation. This then allows the total energy of the reaction process to be calculated, $E_{tot}=E_1+E_2+E_{recoil}$, where $E_{1,2}$ are the kinetic energies of the detected fragments and E_{recoil} is the energy of the unobserved recoil particle. The evaluation of the relative velocity, and in turn the relative energy of the decaying system, enables the excitation energy to be determined.

Figure 2 shows the total energy spectrum for the $^{12}\mathrm{C}(^{10}\mathrm{Be},{}^4\mathrm{He}+{}^6\mathrm{He})^{12}\mathrm{C}$ reaction channel, which has a Q value of −7.4 MeV. The main peak of interest is the one labeled Q_{ggg}, which corresponds to events where all three particles in the exit channel are in their ground states. The background in this spectrum, to the left of the peak, is due to reactions in which either the ^{12}C nucleus is left in a highly excited state or is due to the formation of four-body final states arising from pickup, breakup reactions. The Q_{ggg} peak, which lies at ~290 MeV, is slightly lower in energy than the expected value of 295 MeV (from $E_{tot}=E_{beam}+Q_3$, where Q_3 is the three-body reaction Q value). This difference is due to uncertainties in the calibrations and assumptions made about the energy loss of the beam through the target, corresponding to the uncertainty in the interaction depth within the target.

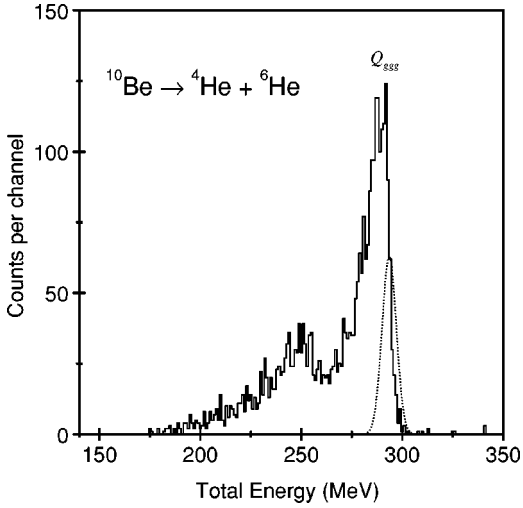

FIG. 2. The total energy spectrum for the reaction ^{12}C(^{10}Be, ^{4}He+^{6}He)^{12}C. The peak labeled Q_{ggg} corresponds to the final state nuclei being in their ground state. The dotted line shows the calculated Q_{ggg} profile.

Using Monte Carlo simulations, taking into account the energy and position resolution of the detectors and the energy loss and energy and angular straggling in the target, indicate that the peak should appear at an energy of 293 MeV. The observed discrepancy suggests that there are residual uncertainties in the calibrations of the CsI detectors. The calibration of the larger angle CsI detectors with the mixed beam was less precise than for the four central detectors, due to difficulties in illuminating the former with the mixed beam. The experimental E_{tot} resolution was found to be ~11 MeV. That predicted by the Monte Carlo simulations which include the uncertainty in the energy calibrations is also 11 MeV (shown in Fig. 2). The observed experimental energy resolution does not allow the various excited states of the recoil particle to be resolved, and thus the spectrum is an integral of all the low-lying states in ^{12}C. This may also contribute to the lower E_{tot} resolution and centroid obtained experimentally.

The presence of several recoil states in the total energy spectrum does not compromise the reconstruction of the ^{10}Be excitation energy spectrum for ^{4}He+^{6}He decays. Figure 3(a) shows the excitation energy spectrum for states in ^{10}Be, generated by selecting events that lie in the Q_{ggg} peak. As noted in Sec. II, the excitation energy resolution is less dependent on the energy as determined by the detector telescopes, but is more sensitive to the position resolution of the detectors and the angular straggling in the target. The Monte Carlo simulations indicate that the excitation energy resolution should be 450 keV at E_x=10 MeV, i.e., much better than that in the E_{tot} spectrum. The spectrum displays two peaks at 9.6±0.1 and 10.2±0.1 MeV, with the former being more strongly populated. The uncertainties quoted here are statistical. Table II lists the various measurements of the levels of the nucleus of ^{10}Be in the excitation energy range of 9.5–10.6 MeV. There are only three states known in this energy range. The peak at 9.6±0.1 MeV is in agreement with a state observed in previous measurements at energies ranging from 9.56 to

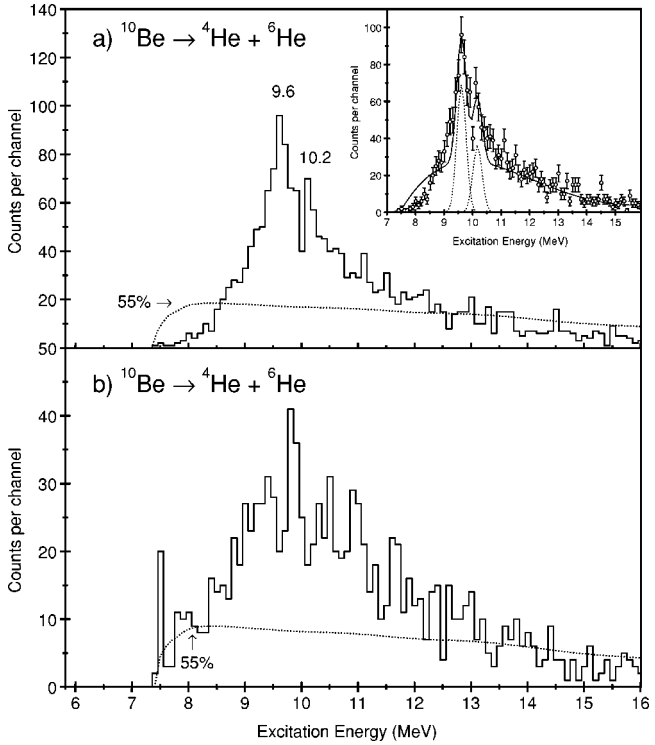

FIG. 3. A comparison between the ^{10}Be excitation energy spectra observed for ^{4}He+^{6}He decays, generated by (a) selecting events that lie in the Q_{ggg} peak in the E_{tot} spectrum and (b) selecting events that lie outside the Q_{ggg} peak. The dotted curve represents the detection efficiency evaluated using Monte Carlo simulations. A maximum efficiency of 55% occurs at around 9 MeV. The inset in (a) shows the fit to the ^{10}Be excitation energy spectrum, described in the text.

9.64 MeV, which was assigned a spin of 2^+ by Curtis *et al.* [7]. The state seen at 10.2±0.1 MeV in the present data may be the state observed by Curtis *et al.* [7] at 10.15 MeV (3^-), and reported at 10.2 MeV by Soić *et al.* [6].

Figure 3(b) shows the ^{10}Be excitation energy spectrum for events in the total energy spectrum falling outside the observed peak. There appears to be no strong evidence for peaks corresponding to excited projectile states in this spectrum. Here, the absence of peaks suggests that the corresponding reactions do not lead to ^{4}He+^{6}He coincidences from the breakup of ^{10}Be, but perhaps result from pickup, breakup reactions [e.g., ^{12}C(**(**^{10}Be, ^{11}Be(^{5}He+^{6}He)**)**^{11}C, Q_3=

TABLE II. ^{10}Be level structure for E_x=9.50–10.60 MeV(where c.m. means center-of-mass).

E_x(MeV)	J^π	$\Gamma_{c.m.}$(keV)	Reference
9.56±0.02	2^+	141±10	[7]
9.6±0.1			[6]
9.64±0.1			[21]
10.15±0.02	3^-	296±15	[7]
10.2			[6]
10.57±30			[18,7,21,6]

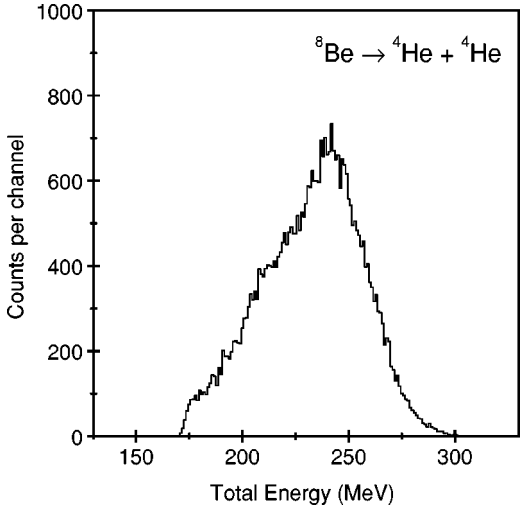

FIG. 4. The total energy spectrum for the $\alpha+\alpha$ coincidences from the ^{10}Be beam, reconstructed assuming a ^{14}C recoil particle.

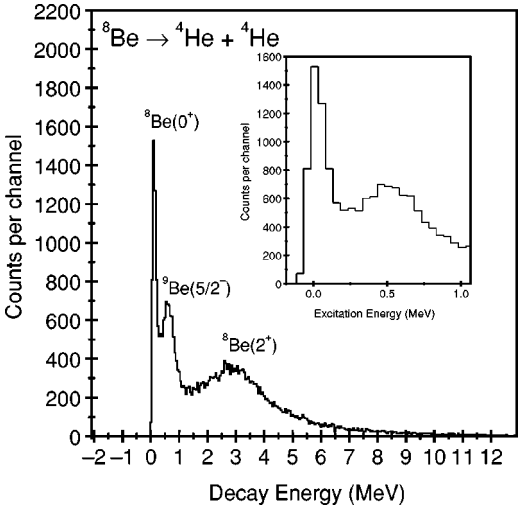

FIG. 5. The decay energy spectrum corresponding to $\alpha+\alpha$ coincidences. The peak at 150 ± 50 keV corresponds to the decay of the ^{8}Be ground state (92 keV). The peak at $\sim$3 MeV is produced by the decay of the first excited state at 3.04 MeV(2^+). The third peak visible at $\sim$630 keV is consistent with the decay of the 2.43 -MeV($5/2^-$) state in ^{9}Be to the low-energy tail of the 2^+ state in ^{8}Be. The inset shows the low-energy part of the ^{8}Be excitation energy spectrum on an expanded scale.

-27 MeV], or those involving the α breakup of the target. Given that the spectrum in Fig. 3(b) appears to correspond to background processes we have made a polynomial fit to these data to determine the peak and background contributions to the spectrum in Fig. 3(a). In this case the background profile has been normalized to the highest-energy part of the spectrum, where there appears to be good agreement with the overall shape of the spectrum [inset in Fig. 3(a)]. On the other hand, for excitation energies close to the decay threshold the agreement is not so good, suggesting that the background processes may vary in nature as a function of E_{tot}. Nevertheless, using the adopted background profile a reasonable agreement is found with the excitation energy spectrum including two peaks at 9.6 and 10.2 MeV, with the theoretical excitation energy resolution. The extracted peak strengths would correspond to inelastic scattering cross sections for the 9.6 and 10.2 MeV states of 0.24(0.02) and 0.13(0.01) mb, respectively.

The angular correlations were reconstructed for the two states observed in the present measurement, following the method described in Ref. [14]. Given that all of the nuclei in the initial and final state are spin zero, then structured correlations could have yielded spin determinations. However, the angular correlations possessed no strong oscillatory patterns and as a consequence no spins could be inferred. This result is in part due to the very large grazing angular momentum in the present reaction ($l\sim38\hbar$) which tends to compress the correlation pattern, which when coupled with limited statistics makes spin assignments difficult. In addition, the above analysis suggests that there may be a significant contribution to the excitation energy spectrum from reactions providing a background.

The detection of two coincident α particles allowed the total energy and excitation energy spectra for the decay of ^{8}Be to be reconstructed. Figure 4 shows the total energy spectrum for $\alpha+\alpha$ coincidences reconstructed assuming a ^{14}C recoil. It is evident from this spectrum that no peak exists at a total energy of 297.5 MeV, even though the experimental resolution was estimated to be similar to the ^{6}He$+\alpha$ channel. In addition, it is possible to state that there is no observable $2n$ transfer yield to low-lying states in ^{14}C. This is in contrast to the ^{12}C(^{12}Be, ^{10}Be*)^{14}C reaction, where a cross section of 0.2–0.6 mb was observed [10].

The source of the high-energy α particles ($\langle E_\alpha\rangle \simeq 30$ MeV/nucleon) is believed to arise predominantly from $2n$-removal (or knockout) reactions, i.e., $2n$ removal from the ^{10}Be beam. Given that, on average, each neutron removes an energy which corresponds to the emission of a neutron with beam velocity, then it is expected that each neutron removes $\sim$30 MeV. Thus, the total energy spectrum should be shifted to lower energies by $\sim$60 MeV ($E_{tot}=237$ MeV). The peak intensity in Fig. 4 lies at $E_{tot}=240$ MeV, in close agreement. Gating on all the yield in this E_{tot} spectrum allowed the decay energy spectrum of ^{8}Be to be reconstructed, as shown in Fig. 5. The strongly populated state at 150 ± 50 keV corresponds to the ^{8}Be ground state, which has a known decay energy of 92 keV, and similarly, the broad state at $\sim$3 MeV is produced by the decay of the first excited state, $E_x=3.04$ MeV(2^+). There is a third peak at an excitation energy of 500 keV which does not coincide with any known state in ^{8}Be, but it is believed to correspond to the decay of the 2.43 MeV ($5/2^-$) state in ^{9}Be to the low-energy tail of the broad 2^+ state in ^{8}Be. The available energy in the ^{9}Be($5/2^-$) decay to ^{8}Be$+n$ is 0.75 MeV and given the small, $l=1$, centrifugal barrier for the ^{9}Be($5/2^-$)$\rightarrow{}^8$Be(2^+)$+n$ decay, yield should extend up to 0.75 MeV as observed in the present data. Indeed, previous studies of the neutron decay of the 2.43 MeV state [15,16], suggest that due to the $l=3$ barrier for the decay to the ^{8}Be ground state, this branch is only 6%–8% of that to the 2^+ state. Measurements of the neutron energy spectra [15] suggest that for the decay from the

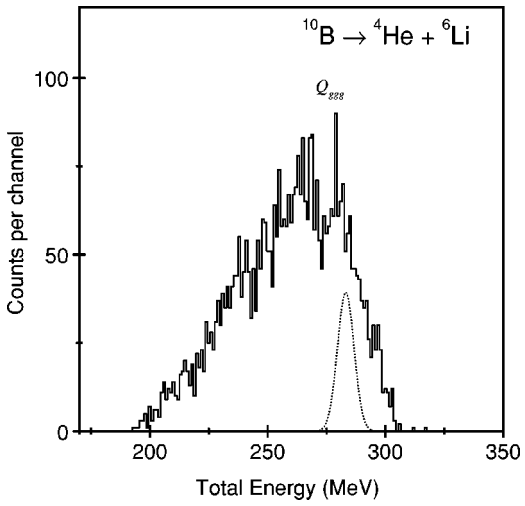

FIG. 6. The total energy spectrum for the reaction ^{12}C(^{10}B,^{4}He+^{6}Li) reconstructed assuming a ^{12}B recoil. The Monte Carlo simulation of the Q_{ggg} profile for the ^{12}C(^{10}Be,^{4}He$_{g.s.}$ +^{6}Li$_{g.s.}$)^{12}B$_{g.s.}$ reaction is shown as a dotted line.

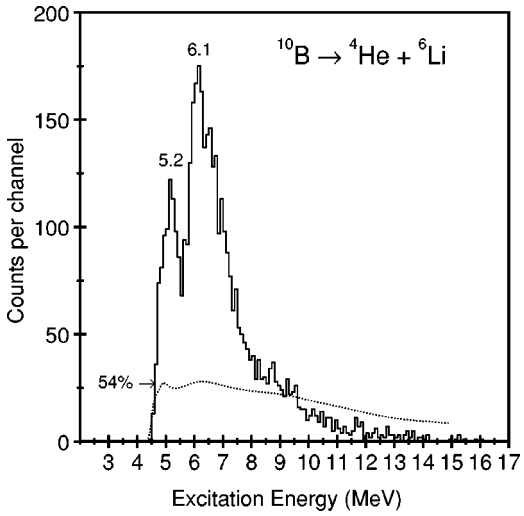

FIG. 7. The excitation energy spectra observed for the decay of ^{10}B into ^{4}He+^{6}Li, generated by selecting all the events in Fig. 6. The dotted curve represents the detection efficiency evaluated using Monte Carlo simulations.

2.43 MeV state to ^{8}Be (2^{+}) gives a mean neutron energy of 300 keV, which is well reproduced with calculations [15,17] in which the α-α final state interactions are included. This mean energy would imply a mean excitation in ^{8}Be of ~450 keV, which when convolved with the experimental resolution is consistent with the present measurement.

The presence of the remnant of the ^{9}Be excited state in the ^{8}Be decay spectrum demonstrates that at least a fraction of the yield proceeds via a sequential process—single-neutron knockout/removal to unbound states in ^{9}Be which subsequently decay—as opposed to direct two-neutron knockout. Indeed, the fact that the majority of the counts in the reconstructed excitation energy spectrum appear to coincide with known states in ^{8}Be indicates that contributions from transfer processes leading to complex multiple body (greater than three particle) final states producing α particles not associated with ^{8}Be decay is small.

Boron isotopes are produced by either the transfer of a proton to the ^{10}Be beam or alternatively, via charge-exchange processes. Figure 6 shows the total energy spectrum for the breakup reaction ^{12}C(^{10}Be,^{4}He+^{6}Li), reconstructed assuming a ^{12}B recoil. The ground-state Q value for this reaction is −17.3 MeV, so the Q_{ggg} peak should lie at ~285 MeV. Monte Carlo simulations, taking into account the energy loss in the target, suggest that a peak at 280 MeV would be expected. However, only a small peak is observed at this energy, analysis of which demonstrates to be feed-through of ^{7}Li+α coincidences (see later). Thus, there is no yield which may be unambiguously identified with the charge-exchange process. The broad distribution below this region is believed to correspond to reaction processes such as proton pickup to form excited states in ^{11}B. These states then decay to ^{7}Li*+α, with the ^{7}Li* decaying by neutron emission; in this case a continuous background would be produced in the ^{4}He+^{6}Li relative energy spectrum. Alternatively, if the ^{11}B excited states decay by neutron emission to α-decaying excited states in ^{10}B, then peaks should be observed in the relative energy spectrum.

Figure 7 shows the excitation energy spectrum generated for ^{10}B, produced by gating over all events in the E_{tot} spectrum. The peak observed at 5.2±0.1 MeV in the excitation energy spectrum is in reasonable agreement with the known α-decaying states at 5.18 MeV(2^{+}) and 5.11 MeV(2^{-}) [19]. The peak at 6.1±0.1 MeV seems to be in good agreement with previous work, as shown in Table III, where an excited state at 6.13 MeV has been assigned a spin of 3^{-} [19], although given the present resolution it is not possible to exclude contributions from the 6.03 MeV(4^{+}) and 5.92 MeV(2^{+}) states. There is possibly a further peak present at E_x=6.5±0.1 MeV, which would coincide with the known 6.56 MeV(4^{-}) state [19]. Beyond 7.5 MeV there is an absence of strongly populated states.

There is a potential ambiguity in the ^{10}B excitation energy spectrum due to the possibility that the ^{6}Li* 3.56 MeV, T =1, state is populated in the decay, a process which could not be identified owing to the nature of the E_{tot} spectrum. In this case the energies of the three observed peaks would then be 3.56 MeV high in energy and would then correspond to the decay of T=1 states in ^{10}B. There is no strong correlation

TABLE III. ^{10}B level structure for E_x=4.70–6.90 MeV [19].

E_x(MeV±keV)	J^{π}	$\Gamma_{c.m.}$(keV)
4.77±0.5	3^{+}	8.7±2.2 eV
5.11±0.6	2^{-}	0.98±0.07
5.18±10	1^{+}	110±10
5.92±0.6	2^{+}	6±1
6.03±0.6	4^{+}	0.05±0.03
6.13±0.7	3^{-}	2.36±0.03
6.56±1.9	4^{-}	25.1±1.1
6.87±5	1^{-}	120±5

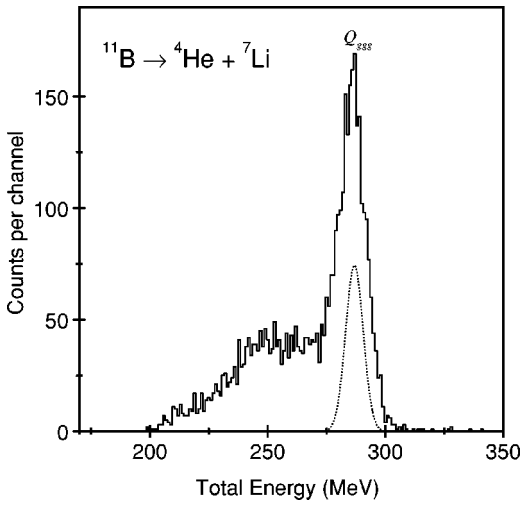

FIG. 8. The total energy spectrum for the decay of ^{11}B into ^{4}He+^{7}Li from the reaction ^{12}C(^{10}Be, ^{11}B*)^{11}B. Monte Carlo simulations of the experimental resolution are shown by the dotted line.

with known excited states in ^{10}B with this character, suggesting that this is not the dominant decay mode. Nevertheless, some contribution from decays to the ^{6}Li(3.56 MeV) excited state may be present in the excitation energy spectrum.

The final two-body decay channel that possessed significant yield was the decay of ^{11}B into ^{4}He+^{7}Li, produced in the ^{12}C(^{10}Be, ^{11}B*)^{11}B reaction. The Q value for this process is −13.4 MeV, which corresponds to the peak at 287 MeV in

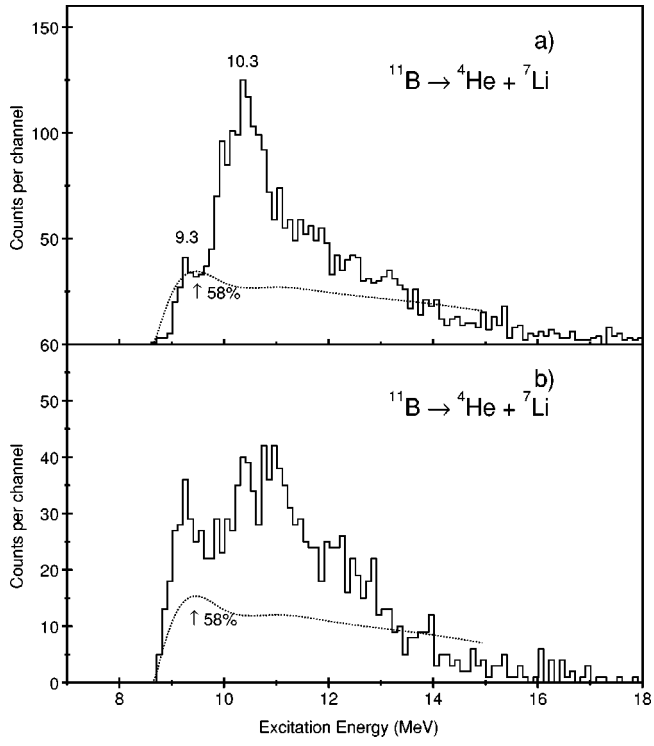

FIG. 9. A comparison between the excitation energy spectra for ^{11}B, generated by (a) selecting events which lie in the Q_{ggg} peak and (b) selecting events that lie below this peak. The dotted curve represents the detection efficiency evaluated using Monte Carlo simulations.

TABLE IV. ^{11}B level structure for E_x=9.1–10.6 MeV [20].

E_x(MeV)	J^{π}	$\Gamma_{\text{c.m.}}$(keV)
9.19±2.0 keV	$7/2^{+}$	$1.9^{+1.5}_{-1.1}$ eV
9.27±2.0 keV	$5/2^{+}$	4
9.88±8 keV	$3/2^{+}$	110±15
10.26±15 keV	$3/2^{-}$	165±25
10.33±11 keV	$5/2^{-}$	110±20
10.60±9 keV	$7/2^{+}$	100±20

the E_{tot} spectrum (Fig. 8), again in good agreement with the Monte Carlo simulations. The excitation energy spectra were generated by gating on the peak [Fig. 9(a)] and by gating on the yield in the total energy spectrum below the peak [Fig. 9(b)]. The similar structure of these two spectra indicates that the lower-energy portion of the total energy spectrum is also due to the breakup of ^{11}B. The peaks observed at 9.3±0.1 and 10.3±0.1 MeV are consistent with known states (Table IV) at 9.19($7/2^{+}$) and 9.27 MeV($5/2^{+}$) for the 9.3 MeV peak and 10.26($3/2^{-}$) and 10.33 MeV ($5/2^{-}$) for the 10.3 MeV peak [20]. The estimated resolution is 450 keV, which suggests, given the 800 keV width of the 10.3 MeV peak, that it may also contain a contribution from the 10.6 MeV($7/2^{+}$) and 9.88 MeV($3/2^{+}$) states. As in the case of ^{6}Li, ^{7}Li possesses a particle-bound excited state at an energy of 0.48 MeV($1/2^{-}$). Decays to this excited state would thus correspond to excitations of ^{11}B at 9.9 and 11.0 MeV. There is a possible candidate for the 9.9 MeV peak at 9.88 MeV($3/2^{+}$), but the counterpart for the 11.0 MeV peak, 10.96 MeV($5/2^{-}$), possesses a width of 4.5 MeV and therefore cannot correspond to the present peak. Thus, it would appear likely that the decay spectrum is dominated by decays to the ^{7}Li ground state. In Fig. 9(b) there is an additional peak at 10.9(0.1) MeV which may perhaps correspond to the decay of a state in ^{11}B at ~11.5 MeV via the first excited state in ^{7}Li.

The cross sections deduced for the breakup channels discussed here are listed in Table V. These cross sections should be regarded as upper limits, as there may be some contribution to the excitation energy spectra from background processes, not identified here. The cross sections are quoted for the total breakup yield and that associated with the peaks observed in the total energy spectra. The principle contribu-

TABLE V. Cross sections deduced for the various breakup channels.

Breakup channel	Cross section (mb) Peak	Total
$^{10}Be^{*} \rightarrow {}^{6}He + \alpha$	1.20(0.03)	2.74(0.05)
$^{10}Be^{*} \rightarrow {}^{8}Be_{g.s.} \rightarrow \alpha + \alpha$	7.97(0.4)	
$^{10}Be^{*} \rightarrow {}^{9}Be(5/2^{-}) \rightarrow \alpha + \alpha$	7.32(0.3)	
$^{10}Be^{*} \rightarrow {}^{8}Be(2^{+}) \rightarrow \alpha + \alpha$	21.6(1.1)	
$^{10}B^{*} \rightarrow \alpha + {}^{6}Li$		3.60(0.06)
$^{11}B^{*} \rightarrow \alpha + {}^{7}Li$	1.72(0.04)	3.65(0.06)

tion to the uncertainties quoted arises from estimates of the detection efficiency.

IV. DISCUSSION

A. ^{12}C(^{10}Be,^{8}Be)

Given that the total cross section for the production of states in ^{8}Be decaying into two α particles (36.9 mb) is an order of magnitude larger than the resonant breakup cross section of ^{10}Be into ^{4}He+^{6}He and the absence of a peak corresponding to the transfer process, it is likely that the dominant process leading to the formation of ^{8}Be is that of direct breakup, or knockout, e.g., as in Ref. [22]. The presence of the ^{9}Be $(5/2^{-})$ decay to the tail of the ^{8}Be(2^{+}) state is a signature of this decay process proceeding sequentially, rather than via single-step removal of the two neutrons. It is probable that the other states observed in the ^{8}Be spectrum are produced via the decay of intermediate states in ^{9}Be. Nevertheless, it is clear that the dominant decay process is to the first excited state in ^{8}Be($\sigma=28.9\pm1.4$ mb), rather than to the ground state ($\sigma=7.97\pm0.40$ mb) by a factor of 3–4. We note that this is not due to the differing detection efficiencies as the cross sections have been corrected for this variation in detection efficiencies for the three peaks. The efficiency for the detection of the decay into the 2^{+} state in ^{8}Be and the $(5/2^{-})$ state in ^{9}Be is 44%, and the efficiency for the decay into the 0^{+} state in ^{8}Be is 22%. The latter efficiency is smaller than for the 2^{+} state owing to a larger probability that two α particles enter a single-CsI crystal for the decay of the ^{8}Be ground state, corresponding to the lower relative velocity of the two α particles.

Given the $3/2^{-}$ spin and parity of the ground state of ^{9}Be, the ground state of ^{10}Be should be dominated by the last two neutrons in a $(p_{3/2})^2$ configuration. Admixtures of other configurations will also be present, for example, ones in which two neutrons occupy the $p_{1/2}$ orbit. Shell-model calculations indicate that the first three states in ^{10}Be correspond predominantly to $0\hbar\omega$ configurations [23,24]. The recoupling of the two $p_{3/2}$ protons in part produces the 3.37 MeV(2^{+}) excitation (other contributions can come from the recoupling of the neutrons if the ground state possesses vacancies in the neutron $p_{3/2}$ orbit), and the promotion of a neutron to the $p_{1/2}$ orbit gives rise to a second 2^{+}, $0\hbar\omega$, state. The first 2^{+} state in ^{8}Be (3.04 MeV) is at a very similar energy to that in ^{10}Be, and can in part be described by the recoupling of the protons (again ignoring the neutron single-particle configuration). The present data would suggest that this recoupling plays an important role in the $2n$-removal process, given the strength of the 2^{+} excitation in ^{8}Be. Evidence for this is also found in the presence of the intermediate ^{9}Be $(5/2^{-})$ state, which again requires the recoupled $p_{3/2}$ protons coupled to the unpaired $p_{3/2}$ neutron to give a $5/2^{-}$ state.

These data demonstrate that at an incident energy of $\sim$30 MeV per nucleon, two-neutron removal reactions in which the core becomes excited dominate. It is known from inelastic scattering measurements for ^{9}Be [25–27] and ^{10}Be [28] that large deformation lengths are required to describe the inelastic excitation probability for these nuclei; 1.61–2.13 fm for ^{9}Be and 1.84–1.99 fm for ^{10}Be. A recent analysis of the one-neutron knockout from ^{11}Be [29] attempted to include the ^{10}Be core rotational excitation using a value of $\beta_2=0.67$. The inelastic excitation was suggested to contribute only $\sim$20% of the total ^{10}Be(2^{+}) excitation, the rest was attributed to $l=2$ configurations within the ^{11}Be ground state. These measurements were, however, performed at 60 MeV per nucleon. Nevertheless, it is clear that in systems in which the projectile and possibly the core (^{8}Be or ^{9}Be) are deformed, then rotational excitations are an important component and feature strongly in the neutron removal process.

B. ^{12}C(^{10}Be,^{10}Be*)

Two excitations are observed in the present measurements which may be identified as the ^{10}Be excited states at 9.6 MeV(2^{+}) and 10.2 MeV(3^{-}). There appears to be no evidence for the inelastic excitation (followed by breakup) of a 4^{+} member of a deformed rotational band built on the ground state, as predicted, for example, by the antisymmetrized molecular dynamics (AMD) [5], molecular orbital [3], and microscopic cluster model [4] calculations. Based upon extrapolations of the 0^{+}, 6.719 MeV, and 2^{+}, 7.542 MeV, states, the 4^{+} state should lie in the excitation energy region of 10–12 MeV. This feature would point to a shell model rather than cluster description of the ^{10}Be ground and first 2^{+} state.

It is worth noting that in fact there is no evidence for other states observed at higher energies in this nucleus via the ^{9}Be(^{9}Be,^{10}Be) [8], ^{12}C(^{15}N,^{17}F)^{10}Be [9], and ^{7}Li(^{7}Li,^{4}He+^{6}He) reactions [7]. States have previously been observed in these reactions at 10.8, 11.8, 13.8, 14.8, and 15.3 MeV. The failure to populate these higher-energy states may reflect their probable higher spins [8] as the present reaction is well matched for the excitation of low-spin states in this excitation energy region. Alternatively, the absence of these states may be related to their structural difference to that of the ^{10}Be ground state, which would lead to small excitation probabilities in inelastic scattering. Such states are distinguishable in, for example, the transfer of a single neutron onto ^{9}Be [8], a nucleus which has a well developed cluster structure in the ground state [1,2]. These observations would point to the similarity of the 9.6(2^{+}) and 10.2 MeV(3^{-}) states to the ground state. In measurements of the α-decay widths of the 7.54 and 9.6 MeV(2^{+}) states [11], the lower-energy state was found to have a marked cluster structure, which appeared to be suppressed for the 9.6 MeV state, consistent with the present interpretation. Shell-model calculations [24] do find evidence for a series of $0\hbar\omega$ states (including a 2^{+}) close to 9 MeV, however, cluster models [3,4] also produce a 2^{+} state at this energy. In summary, it would appear that the 9.6 and 10.2 MeV states are structurally closely related to the ground state and consequently do not exhibit a well developed cluster structure.

C. ^{12}C(^{10}Be,^{10}B*)

The sequence of peaks observed in ^{10}B (5.2, 6.1, and 6.5 MeV) corresponds closely with those observed in the α

decay of $^{10}B^*$ (see, for example, Ref. [30]) at 4.77 MeV, [5.11, 5.18 MeV], [5.92, 6.02, 6.13 MeV], 6.56, and 6.87 MeV, where brackets indicate groups of states that were unresolved in Ref. [30]. The three dominant peaks in the present measurements may be identified with three of these groups, and the presence of the 6.87 MeV state cannot be excluded in the current data. There appears to be little evidence of the 4.77 MeV state in the present data, although this is in a region in which the detection efficiency falls rapidly to zero. The decay to the ground state of ^{6}Li would preclude the population of $T=1$ states in the present measurement.

It is difficult to draw definitive conclusions from the present data given that it is not possible to unambiguously identify which states are involved in the decay process. Nevertheless, it may be noted that the region in which the decay strength is located, which is a region in the shell-model description where the positive parity states (4.77 MeV$[3^+]$, 5.92 MeV$[2^+]$, 6.02 MeV$[4^+]$) are predominantly associated with $0\hbar\omega$ excitations [24]. These are related to single-particle configurations in which, for example (given the symmetry between the protons and neutrons), a valence proton occupies the $p_{1/2}$ orbit and couples to the unpaired $p_{3/2}$ neutron, with the two remaining core protons coupled to produce a spin of 2. In this description of the states, the ^{8}Be core would possess a 2^+ configuration, such as observed in the two-neutron removal process above. We note that $2\hbar\omega$ configurations are predicated by the shell model [24] to lie above the present states. That is to say, the present measurements find no evidence for the population and decay of such states.

It is possible to speculate why the E_{tot} spectrum for the $\alpha+^6$Li coincidences appears to be significantly different from that for $\alpha+^7$Li events. It might be anticipated that the charge-exchange reaction cross section should be approximately one order of magnitude less than that for $1p$ transfer, and indeed this would appear to be the case given the small peak intensity observed in Fig. 6, but as observed in Table V, the total cross sections are of a similar order of magnitude. This would suggest that the population of the states in ^{10}B is being enhanced by other mechanisms. For example, one-proton transfer followed by neutron decay could lead to the population of excited states in ^{10}B. The cross section for the decay of ^{11}B to ^{7}Li$+\alpha$ provides an indication of the strength with which states are populated in the vicinity of the neutron decay threshold ($E_{thresh}=11.45$ MeV). The presence of the large continuum in the ^{10}B total energy spectrum is consistent with such a mechanism, and for a neutron emitted with beam velocity this would indicate that the bulk of the yield should lie at 255 MeV, close to that observed experimentally.

D. ^{12}C(^{10}Be, ^{11}B*)

The peaks in the ^{11}B breakup spectrum coincide with $9.19(7/2^+)$and $9.27\,\mathrm{MeV}(5/2^+)$ states for the peak at 9.3 MeV and $10.26(3/2^-)$ and $10.33\,\mathrm{MeV}(5/2^-)$ for the peak at 10.3 MeV. Both of these have been observed in the α-decay channel [20]. Single-proton transfer onto ^{10}Be would be expected to strongly populate $J^\pi=5/2^+$, $3/2^+$ states for proton transfers into an $l=2$ orbit and $J^\pi=3/2^-$, $1/2^-$ for transfers into an $l=1$ orbit. This may favor the 9.27 and 10.26 MeV states. However, if as seen in the case of ^{8}Be and ^{10}B, there is some significant rearrangement of the ^{10}Be core within the p shell, the other two states may provide significant contributions. The present measurement cannot offer a definitive conclusion owing to the limited energy resolution.

Returning to Figs. 9(a) and 9(b), there is evidence that not only does breakup from ^{11}B to ^{7}Li$+\alpha$ proceed directly following one-proton transfer, but that more complex processes are also present, similar to the case of the breakup of ^{10}B, although their strength, judging by the total energy spectrum is less significant than in the case of ^{10}B. For example, it is possible that states in ^{11}B could be populated by deuteron pickup followed by neutron decay. If this scenario is correct, i.e., the low total energy yield corresponds to higher order processes, then the spectrum of ^{11}B states populated in this manner appears to be similar to that observed in the proton pickup. Such processes need not be complete transfer, but may be related to mechanisms such as transfer to the continuum [31]. At intermediate energies such as those of the present work it has been demonstrated that transfer is well matched for continuum states [31] that lead to cross sections in excess of transfer to bound states. These studies have been made predominantly for stripping reactions, but the present measurements indicate that (at least) for the case of the boron isotopes, the reaction mechanism is complex involving both single-step and transfer-breakup processes.

V. SUMMARY AND CONCLUSIONS

The inelastic excitation of ^{10}Be to two states at 9.6 ± 0.1 and 10.2 ± 0.1 MeV has been observed using a 302 MeV ^{10}Be beam incident on a ^{12}C target. These excitations may be identified with known states at $9.6(2^+)$ and $10.2\,\mathrm{MeV}(3^-)$. In the present measurements there is no evidence for additional states including the proposed [3,4] 4^+ member of a ground state rotational cluster band. This would point to a shell-model-like structure for the ground state. As a consequence, the maximum spin the ground-state configuration could support would be 2, as opposed to cluster model predictions which allow higher spins to be generated.

In two-neutron removal leading to states in ^{8}Be a significant fraction of the yield ($\sim$80%) was observed for the ^{8}Be first excited state (2^+), with a much smaller fraction ($\sim$20%) resulting in the formation of the ^{8}Be ground state. The measurements indicate that the decay process contains significant contributions from sequential two-neutron removal proceeding via the $2.43\,\mathrm{MeV}(5/2^-)$ state in ^{9}Be. This unexpected result suggests that configurations in which the two valence $p_{3/2}$ protons couple to a spin of 2 play an important role in the two-neutron removal process.

Reactions leading to the population of α-decaying states in ^{10,11}B were also observed. In the case of ^{10}B the states populated may be related to structures in which the two protons again couple to a spin of 2. Both of these reactions exhibit continuum contributions (less so in the case of ^{11}B) to the final state. The continuum is believed to be related to more complex four or more body, final states. Interestingly,

the continuum also provides evidence for the resonant decay of $^{10,11}B^{*}$. This would suggest that the processes leading to the observed final states are intricate, in part arising from the three-body breakup, but also with a significant fraction of the yield attributable to pickup followed by breakup. It is possible that such pickup processes are strongly matched to continuum states in the resonant nuclei with corresponding large cross sections.

The unexpected fraction of ^{8}Be nuclei formed in the two-neutron removal in the excited, rather than the ground state, may reflect the fact that the reaction mechanism is not one in which the core remains inert but one in which core nucleons participate in the interaction. Given the large intrinsic deformation of the ^{8}Be, ^{9}Be, and ^{10}Be nuclei it is possible that collective (rotational) modes are being excited in the neutron removal process. There are two possible reaction routes which may contribute incoherently. The first would be the inelastic excitation of ^{10}Be followed by neutron removal. Second, the ^{9}Be core may be rotationally excited following the neutron removal from the ^{10}Be ground state. The key to understanding the nature of the excitation process lies in understanding the spectrum of excited states which are populated in ^{9}Be prior to the decay to the α-unbound states in ^{8}Be. Such information may be obtained via the coincident detection of the neutrons.

The present data may thus provide a useful test of models of nucleon knockout (or removal) which have been used to determine the ground-state structure of neutron-rich nuclei, such as the heavier beryllium isotopes ^{11,12}Be [29,22].

ACKNOWLEDGMENTS

We would like to acknowledge enlightening discussions with D. J. Millener in the preparation of this manuscript. The authors are grateful to the technical and operations staff of LPC and GANIL for their support. This work was funded by the EPSRC (UK) and the IN2P3-CNRS (France). Additional financial support was provided by the ALLIANCE programme of the British Council and the Ministère des Affaires Etrangères, and the Human Capital and Mobility Programme of the European Community (Contract No. CHGE-CT94-0056).

[1] W. von Oertzen, Z. Phys. A **354**, 37 (1996).
[2] W. von Oertzen, Z. Phys. A **357**, 355 (1997).
[3] N. Itagaki and S. Okabe, Phys. Rev. C **61**, 044306 (2000).
[4] P. Descouvemont, Nucl. Phys. **A699**, 463 (2002).
[5] Y. Kanada-En'yo, H. Horiuchi, and A. Doté, J. Phys. G **24**, 1499 (1998).
[6] N. Soić, S. Blagus, M. Bogovac, S. Fazinić, M. Lattuada, M. Milin, D. Miljanić, D. Rendić, C. Spitaleri, T. Tadić, and M. Zadro, Europhys. Lett. **34**, 7 (1996).
[7] N. Curtis, D. D. Caussyn, N. R. Fletcher, F. Maréchal, N. Fay, and D. Robson, Phys. Rev. C **64**, 044604 (2001).
[8] N. Ashwood *et al.*, Phys. Rev. C **68**, 017603 (2003).
[9] H. G. Bohlen *et al.*, Phys. Rev. C **64**, 024312 (2001).
[10] M. Freer *et al.*, Phys. Rev. C **63**, 034301 (2001).
[11] J. A. Liendo, N. Curtis, D. D. Caussyn, N. R. Fletcher, and T. Kurtukian-Nieto, Phys. Rev. C **65**, 034317 (2002).
[12] D. Robson, Nucl. Phys. **A204**, 523 (1973).
[13] W. Rae *et al.*, Phys. Rev. C **30**, 158 (1984).
[14] M. Freer, Nucl. Instrum. Methods Phys. Res. A **383**, 463 (1996).
[15] Y. S. Chen, T. A. Tombrello, and R. W. Kavanagh, Nucl. Phys. **A146**, 136 (1970).
[16] P. R. Christensen and C. L. Cocke, Nucl. Phys. **89**, 656 (1966).
[17] C. L. Cocke and P. R. Christensen, Nucl. Phys. **A111**, 623 (1968).
[18] F. Ajzenberg-Selove, Nucl. Phys. **A490**, 1 (1988).
[19] F. Ajzenberg-Selove, Nucl. Phys. **A413**, 1 (1984).
[20] F. Ajzenberg-Selove, Nucl. Phys. **A433**, 1 (1985).
[21] S. Hamada, M. Yasue, S. Kubono, M. H. Tanaka, and R. J. Peterson, Phys. Rev. C **49**, 3192 (1994).
[22] A. Navin, D. W. Anthony, T. Aumann, T. Baumann, D. Bazin, Y. Blumenfeld, B. A. Brown, T. Glasmacher, P. G. Hansen, R. W. Ibbotson, P. A. Lofy, V. Maddalena, K. Miller, T. Nakamura, B. V. Pritychenko, B. M. Sherrill, E. Spears, M. Steiner, J. A. Tostevin, J. Yurkon, and A. Wagner, Phys. Rev. Lett. **85**, 266 (2000).
[23] D. J. Millener, Nucl. Phys. **A693**, 394 (2001).
[24] E. K. Warburton and B. A. Brown, Phys. Rev. C **46**, 923 (1992).
[25] M. N. Harakeh *et al.*, Nucl. Phys. **A344**, 15 (1980).
[26] R. J. Peterson, Nucl. Phys. **A377**, 41 (1982).
[27] S. Roy *et al.*, Phys. Rev. C **52**, 1524 (1995).
[28] D. A. Auton, Nucl. Phys. **A157**, 305 (1970).
[29] T. Aumann *et al.*, Phys. Rev. Lett. **84**, 35 (2000).
[30] P. J. Leask *et al.*, Phys. Rev. C **63**, 034307 (2001).
[31] A. Bonaccorso and D. M. Brink, Phys. Rev. C **44**, 1559 (1991).